Long-term Deflections of Hybrid GFRP/Steel Reinforced Concrete Beams under Sustained Loads

Phan Duy Nguyen [a*], Vu Hiep Dang [b], Ngoc Anh Vu [a], Polikutin Aleksei Eduardovich [c]

[a] Mientrung University of Civil Engineering, 24 Nguyen Du str., ward 7, Tuyhoa city, 620000, Vietnam.

[b] Hanoi Architectural University, Km10 Nguyen Trai str., Thanhxuan, Hanoi, 100000, Vietnam.

[c] Voronezh State Technical University, house 84, 20-let Oktyabrya st., Voronezh, 394000, Russian Federation.

Abstract

One of the solutions to improve the flexural behavior of Glass fiber reinforced polymer (GFRP) reinforced concrete (RC) beams is the addition of tensile longitudinal steel reinforcement. The numerous studies to date on hybrid GFRP/steel RC elements have mainly focused on the static and short-term responses, very little work has been done regarding the long-term performance. This paper presents experimental results of time-dependent deflections of cracked GFRP and hybrid GFRP/steel RC beams during a 330-day-period in natural climate conditions. Three hybrid GFRP/steel and one GFRP RC beams with dimensions 100×200×2000 mm were tested in four-point bending. Different steel reinforcement ratios were used to evaluate the effect of the steel reinforcement on the long-term behavior of the beams. Experimental results show that the immediate deflections are inversely proportional to the additional steel reinforcement. With the same initial instantaneous deflection, the total deflection increases when increasing the steel reinforcement ratio. Also, temperature (T) and relative humidity (RH) significantly affect the long-term deflection of the tested beams. The measured long-term deflections were found to be in good agreement with the theoretical values calculated from the proposed method. However, there was an overestimation when using ACI 440.1R-15 or CSA-S806-12 procedures.

Keywords: GFRP; Hybrid; Concrete Beam; Long-term; Time-dependent; Sustained Load; Deflection.

1. Introduction

With many outstanding advantages, traditional steel reinforcement is widely used for RC structures. However, in cases where non-conductive, nonmagnetic and corrosion-resistant structures are required, steel reinforcement cannot be used. In these cases, fiber reinforced polymer (FRP) can meet the requirements. Commonly used FRPs include Glass (GFRP), Carbon (CFRP), Aramid (AFRP) and Basalt (BFRP). However, the high cost of FRP limits their applications in practice. Compared with CFRP, BFRP and AFRP bars, GFRP bars are cheaper and more widely used, especially for bending elements. Although GFRP bar has high strength, the low modulus of elasticity causes large deflection and cracks [1-4]. Therefore, in order to meet the second limit state requirements, GFRP RC beams are often designed over-reinforced, which increases material and labor cost [5, 6]. Many researchers tried to implement additional steel bars to the tensile zone of GFRP RC beams to increase bending stiffness, thereby reducing deflection, crack width of beams. In this case, the steel reinforcement is located deep inside the section with a large concrete cover to avoid corrosion from the outside environment. As a result, the hybrid GFRP/steel RC beam is formed. In addition, hybrid FRP/steel RC concrete structures can be found in the form of RC structures strengthened with FRP.

Up to now, many studies focus on the short-term behavior of hybrid FRP/steel RC beams under static load. Concerning concrete beams reinforced with FRP, many studies on time-dependent deflections of FRP RC beams were carried out. These researches focused on factors affecting long-term deflections such as environmental condition, level and duration of the sustained loading, strength of concrete, types of FRP bars, reinforcement ratio, etc. Gross et al. [7] investigated the time-dependent behavior of six normal and six high strength concrete beams with a dimension of 121×235 mm reinforced with GFRP for 180 days. The authors reported that the behavior under sustained loading was similar to that of steel RC beams and the effect of additional flexural cracking over time was found to be important. Miàs et al. [8, 9] investigated the long-term deflections of eight GFRP RC beams under sustained load over 150 days. The results exhibited that the influence of the applied level of the sustained load was not significant. This finding was confirmed by Walkup et al. in [10]. In another study, Mias et al. [11] examined the effect of material properties on long-term deflections of GFRP RC beams for a period of between 250 and 700 days and revealed that the material properties significantly affected long-term deflections of tested beams. The test results indicated that the higher the reinforcement ratio and the lower the compressive strength were, the higher the total-to-instantaneous deflection ratio was. The comparisons of the theoretical and experimental long-term deflections indicate that ACI 440.1R-06 or CSA-S806-02 procedures give some differences in prediction. The authors introduced a simplified (rational) method to obtain time-dependent curvatures and deflections of concrete members reinforced with FRP bars. The method has been deduced from general principles based on the Effective Modulus Method [12] and Eurocode 2 [13]. The influence of variations in environmental conditions and the mechanical properties of the materials are taken into account by creep coefficient k_{creep} and shrinkage coefficient k_{sh}. Hall and Ghali [14] experimentally investigated long-term deflections of GFRP RC beams and compared with those of steel RC beams. The test results indicated that under similar test conditions and the same reinforcement ratio, the GFRP-reinforced beams had long-term deflections, due to creep and shrinkage, 1.7 times greater than those of the steel-reinforced beams.

Currently, the long-term behavior of RC beams strengthened with FRP received great attention of researchers. Pelvris and Triantafillou [15] studied the time-dependent behavior of RC beams strengthened with FRP laminates and proposed an analytical model to predict the long-term deflections. They reported that increasing the CFRP area decreased both the immediate and the creep deflections. Similarly, experimental results by Chami et al. [16], El-Sayed et al. [17], Hong [18], Sobuz et al. [19] proved that the presence of externally bonded FRP plates reduced the immediate deflections and was very useful to control the deflection of RC beams subjected to long term service loads. However, research data on the long-term behavior of new-built hybrid GFRP/steel hybrid beams is very limited. This paper aims to partially cover this gap.

The objective of the investigation described in this paper is to clarify the influence of the steel reinforcement ratio and the initial deflection on the long-term deflection of GFRP/steel RC beams under service-load conditions. The effect of T and RH on the long-term deflection of GFRP/steel hybrid beams is also assessed. Based on the experimental results, the compatibility of ACI 440.2R-17 [20] and CAN/CSA S806-12 [21] for hybrid GFRP/steel beams is verified and a methodology for determining the time-dependent deflections of such beams is proposed.

This article is presented in the following structure: Section 2 describes the experimental program on the hybrid GFRP/steel and GFRP beams under sustained loading over time; Section 3 presents test results and discussion of long-term deflections of tested beams and an analysis of the influence of the natural climate condition, longitudinal reinforcements on the development of long-term deflections. Section 4 illustrates a model to estimate the long-term deflections of hybrid RC beams; and the conclusions are given in the final section. The research flow chart is shown in Figure 1.
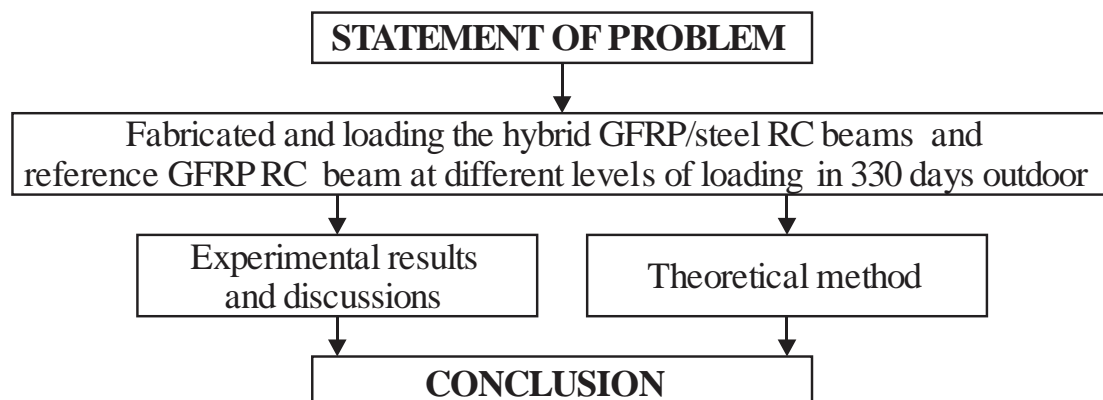

Figure 1. Flow chart of the study

2. Experimental Study

2.1. Specimen Details

The beams were designed as simply supported beams with a rectangular cross-section 100 mm × 200 mm. The total length (l) of the beam was 2000 mm, in which the testing span (l_0) was 1800 mm (Figure 2). The dimension of testing beams was chosen so that they are suitable for the condition and capacity of the available testing facility in the laboratory. The concrete beams reinforced with GFRP and hybrid GFRP/steel reinforcements were designed with reference to ACI 440.1R-15 [6]. All testing beams were designed so that the failure begins by crushing of concrete at the compression side, which is recommended for GFRP RC beam. With the purpose to evaluate the effect of longitudinal steel reinforcements on the time-dependent behavior, the tensile GFRP reinforcement ratio ρ_f of testing beams was fixed while the tensile steel reinforcement ratio ρ_s varied. In testing hybrid GFRP/steel RC beams, the GFRP bar was located lower near the surface with the cover thickness C_f of 15 mm, the steel rebar was located deeper with the cover C_s of 40 mm. Single legged stirrups made from plain steel bar Ø6 were used for testing beams. The tie spacing was taken 100 mm in shear span to avoid shear failure and a 200 mm spacing in midspan. One steel bar Ø6 was used in the compression zone with a concrete cover thickness of 20 mm. Details of testing beams are illustrated in Table 1. The deformed steel bars with diameters of 10 mm, 12 mm, 14 mm and the GFRP bar with a diameter of 14 mm were used as tensile reinforcements. According to the tensile test, the average tensile strength f_f and tensile modulus of elasticity E_f of GFRP bars are 970 MPa and 44300 MPa respectively [22] and the stress-strain diagram is linear until rupture (Figure 3a) [22-24]. The deformed steel bars for tensile reinforcement have average yield strength f_y=412 MPa, ultimate tensile strength f_u=577 MPa and modulus of elasticity E_s=200 GPa and the stress-strain diagrams are shown in Figure 3b.

Table 1. Details of testing beams

Beam ID[a]	Dimensions					Longitudinal reinforcements						
						GFRP reinforcement			Steel reinforcement			Total
	$b \times h$, mm	C_f, mm	C_s, mm	d_{0f}, mm	d_{0s}, mm	Bar	A_f, mm²	ρ_f, %	Bar	A_s, mm²	ρ_s, %	ρ_t, %
B1.G14-S0	100×200	15	-	178	-	1G14	127.6	0.72	-	-	0	0.72
B2.G14-S10	100×200	15	40	178	155	1G14	127.6	0.72	1S10	78.50	0.51	1.23
B3.G14-S12	100×200	15	40	178	154	1G14	127.6	0.72	1S12	113.1	0.73	1.45
B4.G14-S14	100×200	15	40	178	153	1G14	127.6	0.72	1S14	153.9	1.01	1.73

Note: The beam ID is identified by the longitudinal reinforcements, the first symbol shows the sequence number of beams, the second symbol indicates the diameter of the GFRP bar and the third symbol points the diameter of the steel bar, the letter G stands for GFRP and the letter S stands for steel; d_{0f} and d_{0s} – the distances from the centroid of GFRP and steel bars to the outermost compressive concrete fiber, respectively; A_s and A_f – the area of steel reinforcement and GFRP reinforcement, respectively; $\rho_f = A_f/(b \times d_{0f})$ - GFRP reinforcement ratio; $\rho_s = A_s/(b \times d_{0s})$ - steel reinforcement ratio; $\rho_t = \rho_s + \rho_f$ - total tensile reinforcement ratio.
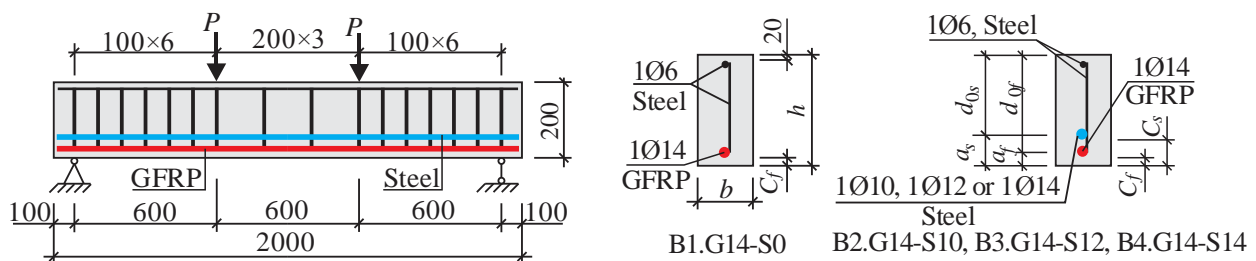

Figure 2. Beam design and loading scheme (unit: mm)

a) GFRP bar   b) Steel bar
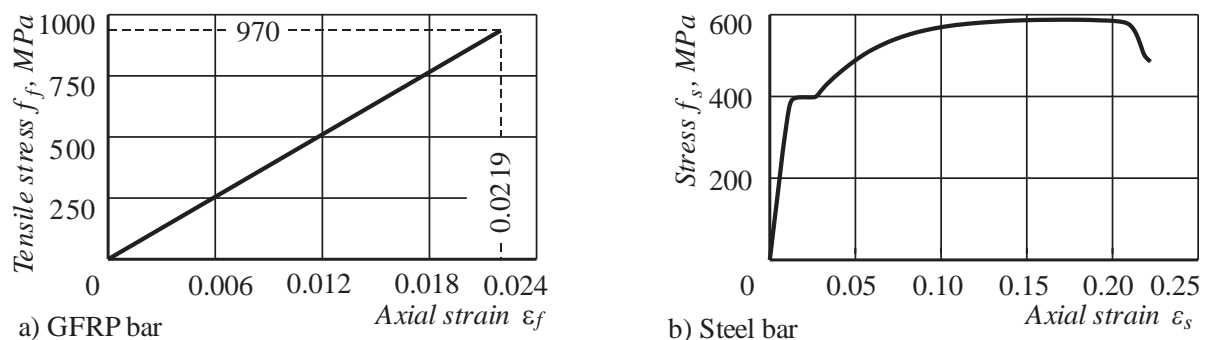
Figure 3. Stress-strain diagram for GFRP bar [22] and steel bar

All beams were prepared from one set of concrete mixture and were removed from the form 24 hours after casting. After that, the beams were cured in water for 7 days and then stored at natural temperatures. The composition for 1m³ of concrete is showed in Table 2. The cubic strength of concretes f_{cu} was determined by testing six cubes of 150 mm×150 mm×150 mm, which were made simultaneously with testing beams. Cylinder strength f_c' and modulus of elasticity E_b of concrete are determined empirically through the cubic strength: $f_c'=0.8f_{cu}$, MPa and $E_b=55000f_{cu}/(27+f_{cu})$, MPa [25, 26].

Table 2. Concrete mix proportion for 1m³

Cement, kg	Sand, m³ (kg)	Gravel, m³ (kg)	Water, lit	Slump, mm	Cube compressive strength f_{cu}, MPa	Cylinder compressive strength f_c', MPa	Modulus of elasticity E_c, MPa
293	0.466 (676)	0.847 (1355)	195	70 mm	40.2	32	32840

2.2. Test Setup and Instrumentation

To reduce the influence of shrinkage, the beam specimens were loaded after 60 days from the end of the curing time. The beams were tested in 4-point bending, in which the loading points were located at 1/3 testing span. First, static loading was performed on the beams to the expected value of deflection. Beams were loaded with dry sandbags and concrete blocks (Figure 4). To avoid the influence of the environmental conditions to the load values, the sand was dried and packed in nylon bags and burlap bags. To assess the effect of the steel reinforcements and the initial immediate deflection on the long-term deflections of the testing beams, the initial deflection of the beams was assumed to be the same. The initial deflection value was chosen on the basis that the corresponding loads cause cracks in the tension zone as well as the steel reinforcement has not yielded yet. The theoretical cracking load (P_{crc}) of GFRP RC beams B1.G14-S0 is equal to 3.3 kN. The sustained load for this beam was chosen $P_{B1}=1.1P_{crc}$ and the corresponding immediate deflections $\delta_0=1.9$ mm. This deflection was chosen for all hybrid GFRP/steel RC beams, the corresponding theoretical load values of beams B2.G14-S10, B3.G14-S12 and B4.G14-S14 are $P_{B2}=1.6P_{crc}$, $P_{B3}=1.8P_{crc}$ and $P_{B4}=2.1P_{crc}$.

Loading on the beams was performed step by step until the deflection reached the expected value for long-term investigation e.g. $\delta_0=1.9$ mm. At each step of loading, the load values and corresponding immediate deflections were recorded. Figure 4 shows the test setup and instrumentation employed to investigate the long-term deflections of hybrid GFRP/steel and GFRP beams under sustained loads. Beam deflections were measured by Dial Indicator Mitutoyo with a resolution of 0.001 mm (Figure 4, 5). The indicator was fixed to the steel support bar (Figure 4, 6), which was welded to two steel supports at both ends of the beam with the purpose to eliminate the displacement of supports during the test.
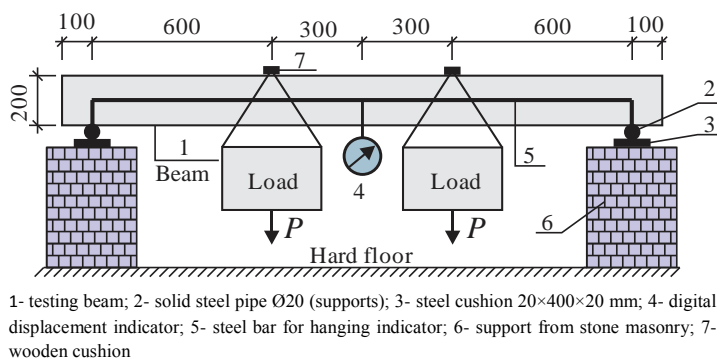

1- testing beam; 2- solid steel pipe Ø20 (supports); 3- steel cushion 20×400×20 mm; 4- digital displacement indicator; 5- steel bar for hanging indicator; 6- support from stone masonry; 7- wooden cushion

Figure 4. Long-term test setup

Temperature and relative humidity at the testing area were hourly recorded by Humidity meter PCE-HT 110 to evaluate the influence of environmental conditions on the long-term deflections of testing beams. The roof and walls were made to protect the testing zone from the impact of the environment around.

3. Results and Discussion

3.1. Short-term Deflection

First, the static tests were performed on all beams until the deflections reached the expected value, $\delta_0=1.9$ mm. The actual load value P applied to each beam is shown in Table 3. The load versus immediate deflection curves of tested beams are shown in Figure 5.
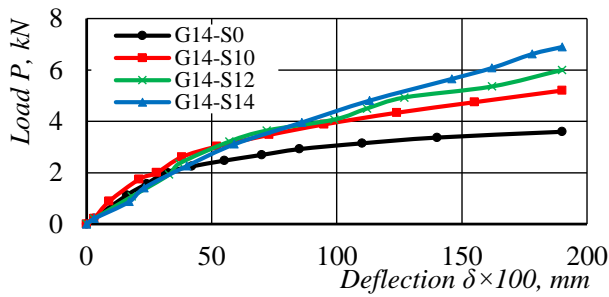
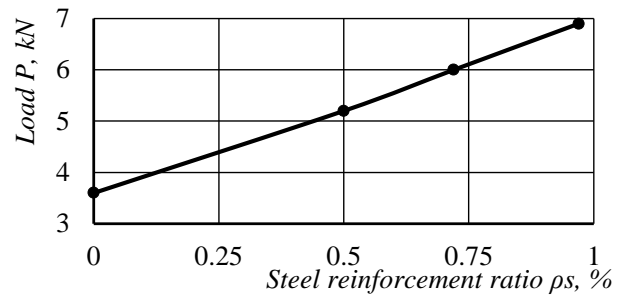**Figure 5. Load versus short-term midspan deflection of testing beams**

Figure 6. Relationship between the steel reinforcement ratio and the applied load at deflection δ=1.9 mm

Before concrete cracks, the role of reinforcements is negligible, therefore the load-deflection relationships of all GFRP and hybrid GFRP/steel beams are almost the same (Figure 5). After cracking of concrete, the development of deflections of tested beams is much different. The steel reinforcement is effective in increasing the stiffness of beams, hence at the same value of load the immediate deflections of hybrid GFRP/steel reduce when increasing the steel reinforcement ratio. Figure 6 shows that the relationship between the steel reinforcement ratio and the load corresponding to the initial short-term deflection of 1.9 mm is almost linear, i.e. the decrease in deflection of hybrid RC beams is inversely proportional to the increase in steel reinforcement ratio.

3.2. Long-term Deflection

After loading the beams to the deflection 1.9 mm, the loads were remained for long-term tests. The test was conducted in natural weather conditions in Tuyhoa city (Phuyen Province, Vietnam) and lasting over 330 days.

In the first 2 days of loading, the deflections of the beams were recorded every half an hour, after that, they were recorded every 24h for two weeks, and then every three days. The T and RH were recorded automatically every hour. Figure 7 presents the long-term deflections of the tested beams, daily average temperature and relative humanity over a 330-day-period.
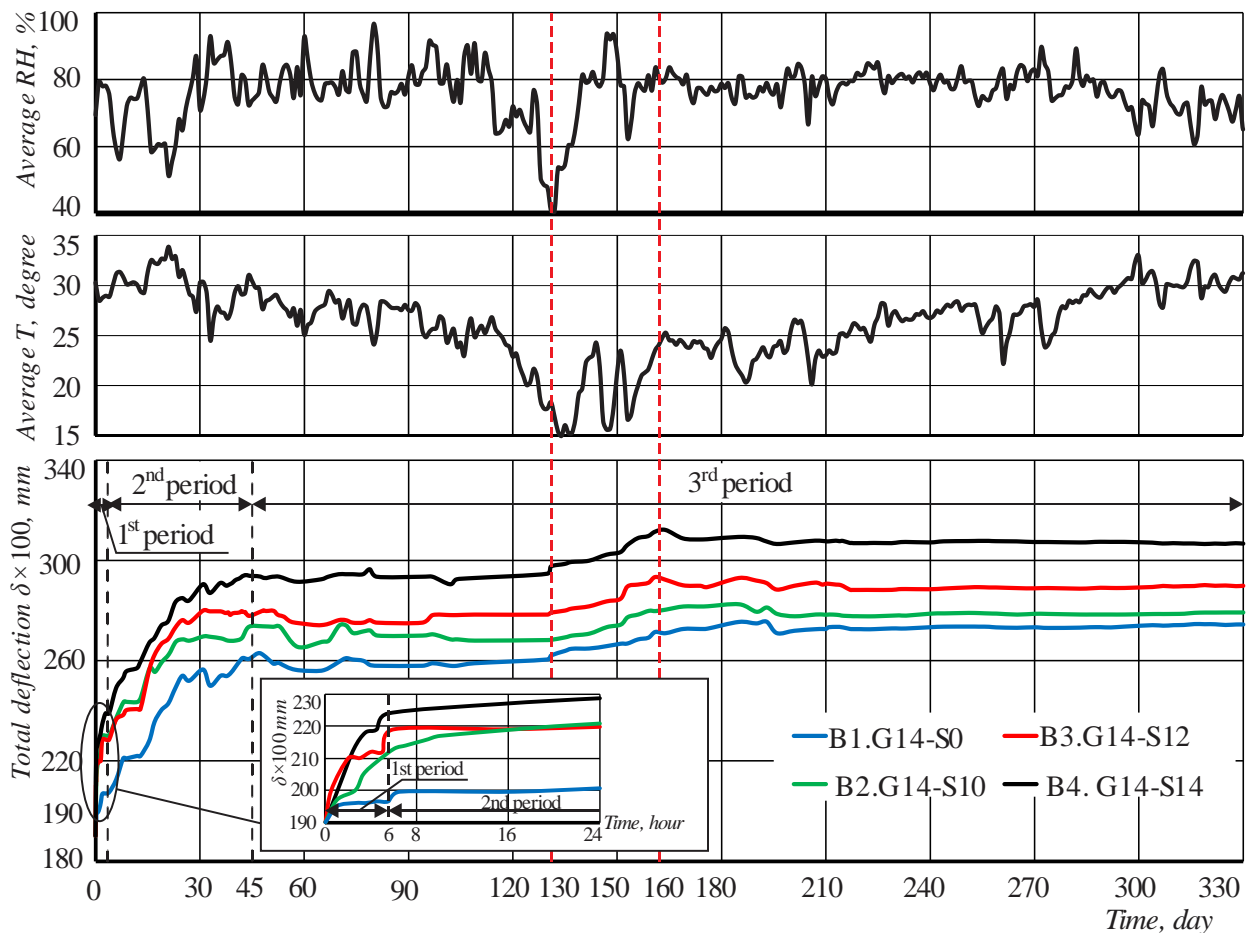

Figure 7. Total deflections of beams with equal initial immediate deflections under sustained loads

As can be observed from Figure 7, the deflection development of GFRP and hybrid RC beams has the same tendency, the creep and shrinkage effects are higher in the initial period and tend to decrease over time. Within 330 days the time-dependent deflection of tested beams could be divided into three periods. During the first some hours after loading (approximately 6 hours), the deflections increase rapidly. After that, the long-term deflections continue increasing, but the increasing rate decreases gradually to nearly 45 days. Beyond 45 days after loading, the long-term deflections increase more slowly and eventually become relatively stable.

It is well known that the creep of concrete is a consequence of the presence of a gel phase in the cement stone, which has high plastic properties. At the initial stage, there is a lot of this gel phase, therefore, the creep of concrete is intensive. Gradually the gel phase becomes consolidated, so the creep deformation descends along with time and then completely stops. Generally, creep deformation of concrete has three stages: primary creep starts rapidly and slows down with time; secondary creep progresses at a relatively uniform rate and tertiary creep. So, in the first period of loading, due to primary creep, shrinkage and possible elongation of GFRP bars the deflections of tested beams rapidly increase. In the early age of loading on beams, the grains of coarse and fine aggregate, grains of cement stone are re-compacted. Depending on the steel reinforcement ratio, the rate of increase in deflection during this period is different. During this period, the total increased in deflections of beams B1.G14-S0, B2.G14-S10, B3.G14-S12 and B4.G14-S14 are (9, 23, 29 and 34)×10-2 mm and account for approximately 11.0, 26.2, 29.0 and 29.0% of the total increase (for 330 day period) respectively. At the end of the first period, the total-to-immediate deflections of four beams B1, B2, B3 and B4 is 1.05, 1.12, 1.15 and 1.18, respectively (Table 3).

Table 3. Deflections of beams at different periods

Beams ID	P, kN	t_0, day	δ_0	t_1, hour	δ_1	$\delta_1-\delta_0$	δ_1/δ_0	t_2, day	δ_2	$\delta_2-\delta_0$	δ_2/δ_0	t_3, day	δ_3	$\delta_3-\delta_0$	δ_3/δ_0
							Total deflections of beams ($\delta_i \times 100$ mm) at different times t_i								
B1.G14-S0	3.6	0	190	6.0	199	9	1.05	45	265	75	1.40	330	272	82	1.43
B2.G14-S10	5.2	0	190	6.0	213	23	1.12	45	274	84	1.44	330	278	88	1.46
B3.G14-S12	6.0	0	190	6.0	219	29	1.15	45	288	98	1.52	330	290	100	1.53
B4.G14-S14	6.9	0	190	6.0	224	34	1.18	45	298	108	1.57	330	307	117	1.62

The second period lasts for about 45 days from the end of the first period. At the end of the first period, the creep of concrete progresses at a relatively constant rate and the long-term deflections of the tested beams mainly depend on creep, shrinkage and environmental conditions. In comparison with the first period, the deflections in the second period develop more slowly. In this period, the development tendency of the deflections of the tested beams is the same pattern. At the 45th day, the deflections due to creep and shrinkage of tested beams (B1…B4) account for 91.5%, 95.8, 98.1 and 92.2% of the total increase observed at the 330th day and the total-to-immediate deflection ratios are 1.40, 1.44, 1.52 and 1.57 respectively (Table 3). Considering the absolute increase ($\delta_2-\delta_1$), the midspan deflections of beams B1, B2, B3 and B4 increase by (70; 68; 77 and 77)×10-2 mm respectively. Thereby, it can be concluded that the effectiveness of steel reinforcement to reduce long-term deflection n in this period is insignificant.

Third period (from the 45th day to the 330th day): with time, the effect of creep and shrinkage of concrete gradually reduces. Therefore, the midspan deflections develop slowly in comparison with the previous periods. During this time, the increase in deflections of B1, B2, B3 and B4 beam accounted for 8.5, 4.2, 1.9 and 7.8% of the total increase in 330 days respectively.

Totally, after 330 days the total deflections of testing beams B1.G14-S0, B2.G14-S10, B3.G14-S12 and B4.G14-S14 increase 43.2, 46.2, 52.6 and 61.7% in comparison with the initial immediate deflection. It is known that the total deflection of the tested beam includes elastic, shrinkage and creep deflections. The increase in the percentage of tension steel reinforcement reduces the shrinkage deflection and increases the creep deflection. In particular, the contribution of the creep deflection to the total deflection is larger than the shrinkage deflection [27]. It should be mentioned that, with the same initial immediate deflection the corresponding sustained loads on testing beams B2.G14-S10, B3.G14-S12 and B4.G14-S14 are 44.4, 66.7 and 91.7% of that of the beam B1.G14-S0. As a consequence, the total deflections of testing beams increase with the increase of steel reinforcement. This finding is consistent with the experimental results by Al Chami et al. (2009) (Beams F5-1-2M10 and F7-1-1M10) [16]. Also, Tan and Saha (2006) [28] carried out a long-term test on RC beams strengthened with FRP and the results showed that the higher the FRP reinforcement ratio, the larger is the long-term deflection under a specific sustained load ratio.

The effect of T and RH on the long-term deflection of RC beams is a complex issue. During the long-term test, the RH varies from 40 to 100 % (average RH is 80 %) and the temperature varies from 15^{0}C to 34^{0}C (Figure 7). The influence of T and RH on the long-term deflections of tested beams is presented by the fluctuation of deflection development curves over time (Figure 7). The influence of these factors is evident in the third period, where the deflections due to the influence of T and RH are remarkable in comparison with the deflections due to creep and

shrinkage. This result is also consistent with the previous research [29]. Specifically, in the high RH period, the increasing rate of long-term deflection decreases, whereas, in the low RH period, the long-term deflection grows rapidly. It can be seen in Figure 7, in the period from 130th to 160th day, the T and RH sharply varied in a wide range, so the deflections considerably grew in comparison with the time intervals before and after this period. It is worth noting that in the monitoring period, the temperature varies in a small range, so the effect of temperature on long-term deflection, in this case, is not clear.

4. Methodology for Predicting Long-term Deflection of Hybrid GFRP/steel RC Beam

4.1. ACI 440.1R-15

ACI 440.1R-15 [6] introduces a simplified equation to predict the long-term deflection of FRP RC beams due to creep and shrinkage. This method is based on the equation for traditional steel RC beams with modifications to take into account the differences in the axial stiffness of the reinforcement for FRP RC beams as compared with steel RC beams. Total deflection (including the creep and shrinkage) of FRP concrete members under bending is computed by equations:

$$\delta_{t(ACI)} = (1 + 0.6\lambda)\delta_0 \tag{1}$$

$$\lambda = \frac{\xi}{1 + 50\rho'} \tag{2}$$

Where: $\delta_{t(ACI)}$ – the total deflection at time t, δ_0 – the immediate deflection caused by the sustained load; $\rho'=A_s'/(bd)$ - the compression reinforcement ratio; ξ - the time-dependent factor for sustained loads, which includes the effects of creep and shrinkage and equals 1.0, 1.2 and 1.4 for 3, 6 and 12 months, respectively. For 5 years or more: $\xi=2$ [25].

4.2. CSA-S806-12 (R2017)

According to CAN/CSA-S806-12 guidelines [30], the total of immediate and long-time deflection for flexural members reinforced with FRP should be obtained by multiplying the immediate deflections caused by the sustained load:

$$\delta_{t(CSA)} = (1 + S)\delta_0 \tag{3}$$

Where: S - the time-dependent factor equals 1.0, 1.2 and 1.4 for 3, 6 and 12 months, respectively. For 5 years or more: $S=2$.

4.3. Proposed Methodology

Experimental data and total deflection predictions according to both ACI 440.1R-15 [6] and CSA-S806-12 [26] are compared in Figure 8. As can be observed in these figures, ACI and CSA overestimate the total deflections. This overestimation is probably due to the time-dependent factor which is calibrated directly for steel FRP RC members. It should be noted that both ACI 440.1R-15 and CSA-S806-12 were developed for beams reinforced with FRP bars only.

The studies carried out by several authors [11, 31] proposed a straightforward methodology to predict long-term deflections of GFRP RC beams based on rational multiplicative coefficients deduced from the principles of the Effective Modulus Method (Eurocode 2). For a simply supported beam, the total deflection can be obtained from the immediate deflection and the multiplicative coefficients k_{creep} and k_{sh}:

$$\delta_{t(proposed)} = \delta_0\big(1 + k_{creep}\big) + \frac{\varepsilon_{sh}(t,t_0)l^2}{8d}k_{sh} \tag{4}$$

Where d is the effective depth; $\varepsilon_{sh}(t,t_0)$ is the free shrinkage strain at age of concrete t (days), measured from the start of loading at t_0 (days), ie, the shrinkage strain from the end of curing time (t_c) to the time of start of loading is not taken into account. According to ACI 209R-92 [32], the free shrinkage strain $\varepsilon_{sh}(t,t_c)$ at age of concrete t (days), measured from the start of drying at t_c (days), can be calculated by Equation 5:

$$\varepsilon_{sh}(t,t_c) = \frac{(t-t_c)^\alpha}{f + (t-t_c)^\alpha}\varepsilon_{shu} \tag{5}$$

Where f (days) and α are considered constants for a given member shape and size that define the time-ratio part; ε_{shu} is the ultimate shrinkage [32].

Coefficient k_{creep} is obtained as follows:

$$k_{creep} = 0.73\phi(t,t_0)\sqrt{n_f\rho_f + n_s\rho_s} \tag{6}$$

Where: $n_f=E_f/E_c$ and $n_s=E_s/E_c$. $\phi(t,t_0)$ is the time-dependent creep coefficient at concrete age t due to a load applied at the age t_0, which can be determined according to ACI 209R-92 [32]:

$$\phi(t,t_0) = \frac{(t-t_0)^{\psi}}{f+(t-t_0)^{\psi}}\phi_u \tag{7}$$

Where: f (days) and ψ are considered constants for a given member shape and size that defined the time-ratio part, ACI 209R-92 recommends an average value of 10 and 0.6 for f and ψ respectively; ϕ_u is the ultimate creep coefficient [32]:

$$\phi_u = 2.35\gamma_c \tag{8}$$

Where γ_c represents the cumulative product of the applicable correction factors [32].

The coefficient k_{sh} depends on the reinforcements and is suggested to determine according to the following equation:

$$k_{sh} = 1 + \sqrt{n_f\rho_f + n_s\rho_s} \tag{9}$$

It is worth mentioning that the Equations 4, 6 and 9 explicitly take into account the effect of environmental conditions and mechanical properties of the materials on the increase of deflection over time. Moreover, the contributions to long-term deflection of creep and shrinkage effects are considered separately.

Figure 8 compares the experimental time-dependent deflections with theoretical time-dependent deflections of hybrid GFRP/steel RC beams obtained according to ACI 440.1R-15, CSA-S806-12 and the proposed method. In calculation by the proposed method, the following parameters are used: time of moist curing t_c=7 days; age of loading t_0=45 days; average temperature T=28[0]C; ambient RH=80%; the air content α=6% (ACI 211.1-91); the ultimate shrinkage strain ε_{shu}=417×10^{-6}.

It can be seen in Figure 8, the development of the theoretical long-term deflections of hybrid RC beams according to ACI 440.1R-15, CSA-S806-12 and the proposed method has a similar tendency but different values. At the time of 330 days, the difference between the experimental and theoretical results is less than 5 %. Meanwhile, CSA-S806-12 and ACI 440.1R-15 overestimate with the average deviation of more than 13 and 54%, respectively in comparison with the experimental results. Besides, as can be seen on Figure 8, in the first period the theoretical and the experimental long-term deflections develop variously with a large difference. This difference may be caused by primary creep, the variation of weather conditions, the elongation of reinforcements, etc.
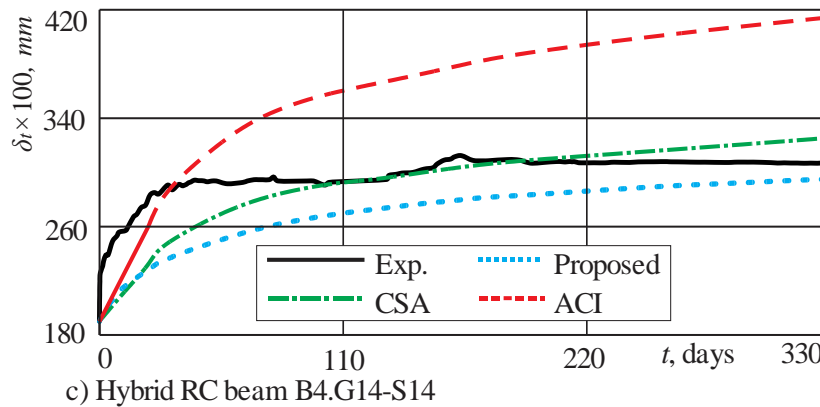

a) Hybrid RC beam B2.G14-S10

b) Hybrid RC beam B3.G14-S12

c) Hybrid RC beam B4.G14-S14
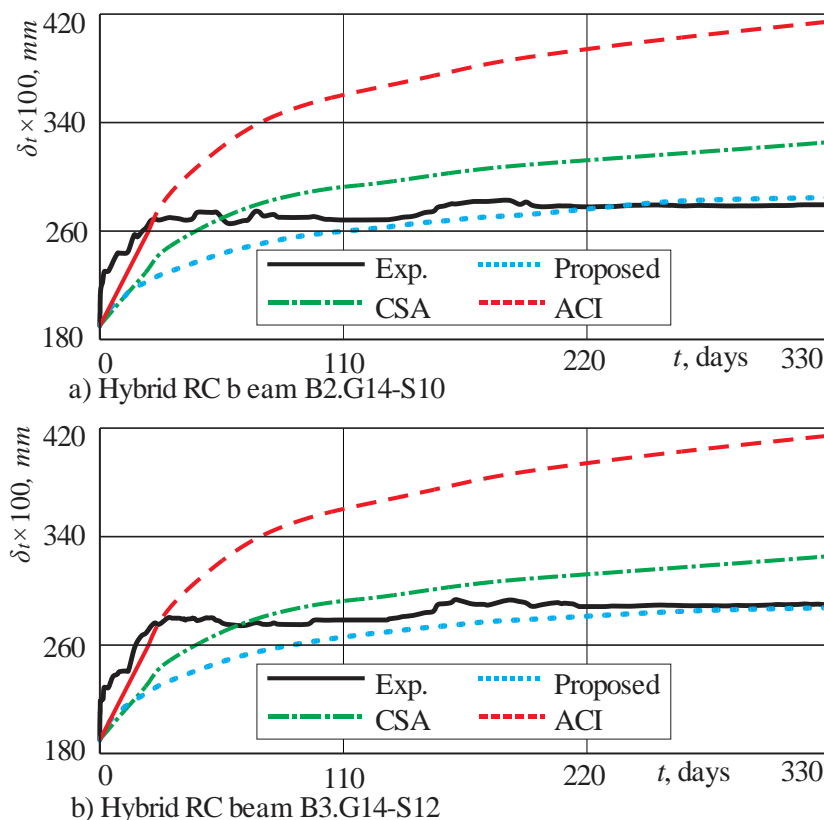
Figure 8. Experimental and theoretical total deflections of hybrid GFRP RC beams

5. Conclusions

This study examines the experimental long-term deflections of hybrid GFRP/steel during 330 days. The recorded results allow identifying three typical stages of development of long-term deflection. Besides, the effects of additional steel reinforcement and environmental conditions on the long-term deflection of the beams are considered. Based on the experimental results presented in this study, the following conclusions can be drawn:

- The development of total deflections of GFRP RC beam and hybrid GFRP/steel beams during the observing time has the same tendency and is divided into three stages;

- The tensile steel reinforcements in hybrid GFRP/steel RC beams significantly reduce the immediate deflections. However, under the same initial immediate deflections, the deflections due to creep and shrinkage of hybrid RC beams increase with the increase of steel reinforcements;

- Using ACI 440.1R-15 and CSA-S806-12 methods for predicting the long-term deflection of hybrid GFRP/steel RC beam gives a remarkable error and too conservative.

- The long-term deflections predicted by Equations 4 to 9 provided better results because these equations take into account the influence of steel and GFRP reinforcement ratio on the creep coefficient, k_{creep}.

It should be noted that the above conclusions are based on the test results carried out on a limited number of specimens and natural climate conditions in Phuyen province, Vietnam. Further research is recommended for studying the effect of material properties, the sustained load levels, environmental conditions on long-term deflections of hybrid GFRP/steel RC beams for a longer duration.

6. Conflicts of Interest

The authors declare no conflict of interest.

7. References

[1] Toutanji, Houssam, and Yong Deng. "Deflection and Crack-Width Prediction of Concrete Beams Reinforced with Glass FRP Rods." Construction and Building Materials 17, no. 1 (February 2003): 69–74. doi:10.1016/s0950-0618(02)00094-6.

[2] Cheung, Moe M.S., and Terry K.C. Tsang. "Behaviour of Concrete Beams Reinforced with Hybrid FRP Composite Rebar." Advances in Structural Engineering 13, no. 1 (February 2010): 81–93. doi:10.1260/1369-4332.13.1.81.

[3] Soric, Zorislav, Tomislav Kisicek, and Josip Galic. "Deflections of Concrete Beams Reinforced with FRP Bars." Materials and Structures 43, no. S1 (April 14, 2010): 73–90. doi:10.1617/s11527-010-9600-1.

[4] Al-Sunna, Raed, Kypros Pilakoutas, Iman Hajirasouliha, and Maurizio Guadagnini. "Deflection Behaviour of FRP Reinforced Concrete Beams and Slabs: An Experimental Investigation." Composites Part B: Engineering 43, no. 5 (July 2012): 2125–2134. doi:10.1016/j.compositesb.2012.03.007.

[5] NIIZHB. "Concrete structures reinforced with fibre-reinforced polymer bars. Design rules (SP 295.1325800.2017)". 2018: Moscow. p. 55.

[6] ACI. "Guide for the design and construction of structural concrete reinforced with FRP bars (ACI 440.1R-15)". 2015, American Concrete Institute.

[7] Gross, Shawn P., Joseph Robert Yost, and George J. Kevgas. "Time-Dependent Behavior of Normal and High Strength Concrete Beams Reinforced with GFRP Bars Under Sustained Loads." High Performance Materials in Bridges (September 5, 2003). doi:10.1061/40691(2003)40.

[8] Miàs, C., Ll. Torres, A. Turon, M. Baena, and C. Barris. "A Simplified Method to Obtain Time-Dependent Curvatures and Deflections of Concrete Members Reinforced with FRP Bars." Composite Structures 92, no. 8 (July 2010): 1833–1838. doi:10.1016/j.compstruct.2010.01.016.

[9] Miàs, C., Ll. Torres, A. Turon, M. Baena, I. Vilanova, and M. Llorens. "Experimental Study of Time-Dependent Behaviour of Concrete Members Reinforced with GFRP Bars." Advances in FRP Composites in Civil Engineering (2011): 352–355. doi:10.1007/978-3-642-17487-2_76.

[10] Walkup, Stephanie L., Eric S. Musselman, and Shawn P. Gross. "Effect of Sustained Load Level on Long-Term Deflections in GFRP and Steel-Reinforced Concrete Beams." International Congress on Polymers in Concrete (ICPIC 2018) (2018): 609–615. doi:10.1007/978-3-319-78175-4_78.

[11] Miàs, C., Ll Torres, A. Turon, and I.A. Sharaky. "Effect of Material Properties on Long-Term Deflections of GFRP Reinforced Concrete Beams." Construction and Building Materials 41 (April 2013): 99–108. doi:10.1016/j.conbuildmat.2012.10.1.055.

[12] Bazant Z.P. "Prediction of Concrete Creep Effects Using Age-Adjusted Effective Modulus Method." ACI Journal Proceedings 69, no. 4 (1972). doi:10.14359/11265.

[13] EUROPEAN COMMITTEE, et al. "Design of Concrete Structures—Part 1-1: General Ruels and Rules for Buildings (EN 1992-1-1 Eurocode 2)". European Committee: Brussels, Belgium, 2005.

[14] Hall, Tara, and Amin Ghali. "Long-Term Deflection Prediction of Concrete Members Reinforced with Glass Fibre Reinforced Polymer Bars." Canadian Journal of Civil Engineering 27, no. 5 (October 1, 2000): 890–898. doi:10.1139/l00-009.

[15] Plevris, Nikolaos, and Thanasis C. Triantafillou. "Time‐Dependent Behavior of RC Members Strengthened with FRP Laminates." Journal of Structural Engineering 120, no. 3 (March 1994): 1016–1042. doi:10.1061/(asce)0733-9445(1994)120:3(1016).

[16] Al Chami, G., M. Thériault, and K.W. Neale. "Creep Behaviour of CFRP-Strengthened Reinforced Concrete Beams." Construction and Building Materials 23, no. 4 (April 2009): 1640–1652. doi:10.1016/j.conbuildmat.2007.09.006.

[17] El-Sayed, Ahmed K., Rajeh A. Al-Zaid, Abdulaziz I. Al-Negheimish, Ahmed B. Shuraim, and Abdulrahman M. Alhozaimy. "Long-Term Behavior of Wide Shallow RC Beams Strengthened with Externally Bonded CFRP Plates." Construction and Building Materials 51 (January 2014): 473–483. doi:10.1016/j.conbuildmat.2013.10.055.

[18] Hong, Sungnam, and Sun-Kyu Park. "Long-Term Behavior of Fiber-Reinforced-Polymer-Plated Concrete Beams Under Sustained Loading: Analytical and Experimental Study." Composite Structures 152 (September 2016): 140–157. doi:10.1016/j.compstruct.2016.05.031.

[19] Ahmed, Ehsan, and Habibur Rahman Sobuz. "Immediate and Long-Term Deflection of Carbon Fiber Reinforced Polymer (CFRP) Concrete Beams." Key Engineering Materials 471–472 (February 2011): 73–78. doi:10.4028/www.scientific.net/kem.471-472.73.

[20] ACI, Guide for the Design and Construction of Externally Bonded FRP Systems for Strengthening Concrete Structures (ACI 440.2R-17). (2017). American Concrete Institute.

[21] ACI. "Guide for the Design and Construction of Externally Bonded FRP Systems for Strengthening Concrete Structures (ACI 440.2R-17)" (May 2017). doi:10.14359/51700867.

[22] Lucier, G. "Tension Tests of GFRP Bars (Prepared for: Fiber reinfor polymer Viet Nam)". (2016). North Carolina State University. p. 7.

[23] R., Balamuralikrishnan, and Saravanan J. "Finite Element Analysis of Beam–Column Joints Reinforced with GFRP Reinforcements." Civil Engineering Journal 5, no. 12 (December 1, 2019): 2708–2726. doi:10.28991/cej-2019-03091443.

[24] Nguyen, Phan Duy, Vu Hiep Dang, and Ngoc Anh Vu. "Performance of Concrete Beams Reinforced with Various Ratios of Hybrid GFRP/Steel Bars." Civil Engineering Journal 6, no. 9 (September 1, 2020): 1652–1669. doi:10.28991/cej-2020-03091572.

[25] ACI. "Building Code Requirements for Structural Concrete (ACI 318-19): An ACI Standard: Commentary on Building Code Requirements for Structural Concrete (ACI 318R-19)". (2019). American Concrete Institute.

[26] Baikov V.N. and Sigalov E.E. "Reinforced concrete structures, General Course: book for higher schools, 5th edition". (1991), Stroyizdat, Moscow.

[27] Shariq, M., H. Abbas, and J. Prasad. "Effect of Magnitude of Sustained Loading on the Long-Term Deflection of RC Beams." Archives of Civil and Mechanical Engineering 19, no. 3 (May 2019): 779–791. doi:10.1016/j.acme.2019.03.004.

[28] Tan, Kiang Hwee, and Mithun Kumar Saha. "Long-term deflections of reinforced concrete beams externally bonded with FRP system." Journal of Composites for Construction 10, no. 6 (2006): 474-482. doi:10.1061/(ASCE)1090-0268(2006)10:6(474).

[29] Li, Pengfei, and Shiqin He. "Effects of Variable Humidity on the Creep Behavior of Concrete and the Long-Term Deflection of RC Beams." Advances in Civil Engineering 2018 (October 29, 2018): 1–12. doi:10.1155/2018/8301971.

[30] CSA. "Design and construction of building components with fiber-reinforced polymers (CSA-S806-12 (R2017))". (2017). Mississauga, Ontario, Canada.

[31] Torres, Ll., C. Miàs, A. Turon, and M. Baena. "A Rational Method to Predict Long-Term Deflections of FRP Reinforced Concrete Members." Engineering Structures 40 (July 2012): 230–239. doi:10.1016/j.engstruct.2012.02.021.

[32] ACI. "Guide for modeling and calculating shrinkage and creep in hardened concrete (ACI 209.2R-08)". (2008): 48p. American Concrete Institute.